PALAIOS
Emphasizing the impact of life on Earth's history

PALAIOS, 2009, v. 24, p. 51–58
Research Article
DOI: 10.2110/palo.2008.p08-013r

DINOSAUR-BEARING ONCOIDS FROM EPHEMERAL LAKES OF THE LOWER CRETACEOUS CEDAR MOUNTAIN FORMATION, UTAH

RUSSELL S. SHAPIRO,[1]* HENRY C. FRICKE,[2] and KELLY FOX[3]
[1]California State University, Geological and Environmental Sciences, Chico, California 95929, USA; [2]Colorado College, Department of Geology, 14 E. Cache La Poudre, Colorado Springs, Colorado 80903, USA; [3]College of Saint Benedict, Department of Geology, St. Joseph, Minnesota 56374, USA
e-mail: rsshapiro@csuchico.edu

ABSTRACT

Here we document the occurrence of locally common oncoids in the Cedar Mountain Formation of Utah in the Woodside Anticline area of the San Rafael Swell and use them to understand changes in the Early Cretaceous landscape and their effects on the dinosaur fauna. Detailed facies analysis is required to understand the context of these changes within the broader patterns of Mesozoic tectonics and the fossil record. Oncolite crops out in the Cedar Mountain Formation, directly overlying the Buckhorn Conglomerate. Oncolite is not widely distributed outside of the Woodside Anticline area. The oncoids are found in a bimodal population with the majority in the 2–5-cm-diameter range and a smaller population >25 cm in diameter. Nuclei are mostly rounded chert clasts and also include litharenite, polymict conglomerate, limestone, and both abraded and nonabraded dinosaur bone and wood fragments. Cortices are 3–5 mm thick with distinct, penecint (laminae that completely enclose a body; Hofmann, 1969), low-relief laminae. Some laminae are crenulated and comprise ministromatolites. The petrography of the oncoids suggests formation along lake margins where large fragments of reworked sedimentary clasts and dinosaur bones came to rest and were coated by bacterial mats. Caliche cements and coats some of the oncolite; these define a lake shoreline affected by fluctuating lake level. The isotope geochemistry indicates a combination of primary and diagenetic signals consistent with oncoid formation in open, ephemeral freshwater lakes.

INTRODUCTION

Oncoids described from the Cedar Mountain Formation (CMF) above the Buckhorn Conglomerate Member (BCM; see Weiss and Roche, 1988) prove useful for landscape reconstruction. Oncoids are unique forms of microbialite broadly defined as coated grains >2 mm diameter, composed of concentric but typically incomplete laminations (Tucker and Wright, 1990). The fossil record of oncoids stretches back into the Archean, and oncoids form today in a number of marine and freshwater locations (e.g., Freytet and Plaziat, 1979; Peryt, 1983; Ratcliffe, 1988; Davaud and Girardclos, 2001). In most cases, oncoids occur in wholly submerged environments, typically of high energy. Common facies include high-energy tidal and river channels, beaches, and lake shorelines (Awramik et al., 2000; Dixit, 1984; Lanes and Palma, 1998; Rouchy et al., 1993). Concentric laminations form when localized microbial ecosystems coat the exposed surfaces of a clast and drive local cementation through microenvironmental changes in water chemistry. The dominant paradigm has been that oncoids accrete on the upper exposed surface because the cyanobacteria responsible for their formation grow toward the sunlight. Additional surfaces become exposed, and laminae accrete, as the growing oncoid flips over during high-energy movement from waves or streams.

Here we describe a deposit of oncoids from the CMF, directly overlying the BCM within the Woodside Anticline of the eastern San Rafael Swell (Fig. 1). The distribution, sedimentology, petrology, and stable isotope geochemistry of these oncolite beds help constrain the paleoenvironments of the lower CMF to further our understanding of the Early Cretaceous basin, east of the Sevier highlands.

The CMF of Utah and western Colorado is recognized as an important record of the tectonic and landscape evolution that took place from Late Jurassic through Eocene time (Weiss and Roche, 1988; Currie, 1998; Demko et al., 2004; DeCelles and Coogan, 2006; Roca and Nadon, 2007). Contrasting tectonic models rely on detailed facies analysis for deciphering landscape denudation in response to uplift and environmental shifts due to basin subsidence during and after the Sevier Orogeny. This time period is also significant as the strata record the change in dinosaur fauna from a transatlantic to a more endemic population (Cifelli et al., 1997; Kirkland et al., 1997, 1998, 1999) and is a major part of the discussion of the interchange of Asian faunas with the Americas (Kirkland et al., 2005; Britt et al., 2006). Of particular note are the enigmatic therizinosaurs, once thought to be Asian in origin but now potentially originating in the United States (Kirkland et al., 2005; Kirkland and Madsen, 2007). Still another emerging facet of this period is the widely variable climate, as recorded by paleosols and spring carbonates (e.g., White et al., 2005; Zakharov et al., 2005; Dumitrescu et al., 2006; Suarez et al., 2007). Understanding the details of the landscape through facies analysis will help model the complex interplay of tectonics, climate, and sedimentation to address these questions better.

The CMF was deposited unconformably on the Upper Jurassic Morrison Formation during the Neocomian?–Albian (Early Cretaceous period), though exact confining ages have yet to be determined (Currie, 1998; Kirkland et al., 2005). Previous and ongoing research into the CMF and equivalent formations has distinguished a variety of sedimentary facies that represent continental environments (Kirkland et al., 1997; Sprinkel et al., 1999). Originally defined by Stokes (1949, 1952) and long thought to be a monotonous sequence of unfossiliferous shales, the CMF is now divided into five members (Fig. 1A; see Kirkland et al., 1997). The different members are defined primarily on grain size and secondarily on distribution (Kirkland and Madsen, 2007).

The basal BCM is up to 25 m thick and confined to one or more major incised valleys (Currie, 1998). The majority of clasts within the BCM consist of Paleozoic-aged chert eroded from emergent mountains to the west. The remaining CMF members contain a variety of floodplain (Yellow Cat, Ruby Ranch, and Mussentuchit Members) and channel deposits (Poison Strip Sandstone). The stratigraphic relationship between these members is poorly constrained, though the Ruby Ranch and Mussentuchit Members are the most widely distributed. In this paper, we follow the stratigraphy of Kirkland and Madsen (2007), though we acknowledge that it is difficult to clearly distinguish the Ruby Ranch Member and Poison Strip Sandstone in this area.

GEOLOGICAL SETTING AND MATERIALS

The Woodside Anticline is a low, south-plunging anticline superposed on the larger, broad Laramide-aged anticline that defines the San Rafael

* Corresponding author.

 0883-1351/09/0024-0051/$3.00

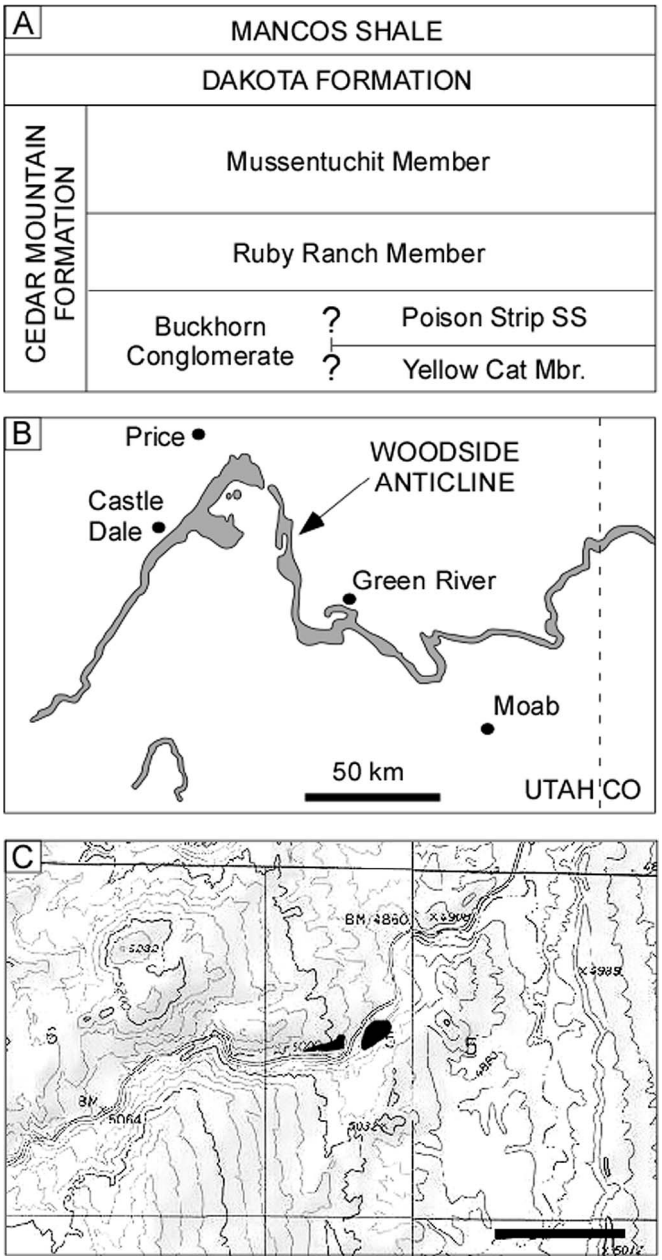

FIGURE 1—The Cedar Mountain Formation in eastern Utah. A) General stratigraphy in the vicinity of the Woodside Anticline. B) Map of the Cedar Mountain Formation in the San Rafael Swell, continuing east into Colorado. C) Outcrop map of the oncolite beds in the Woodside Anticline. Scale bar on map = 1000 m. A and B based on Kirkland and Madsen (2007). SS = sandstone; Mbr = member.

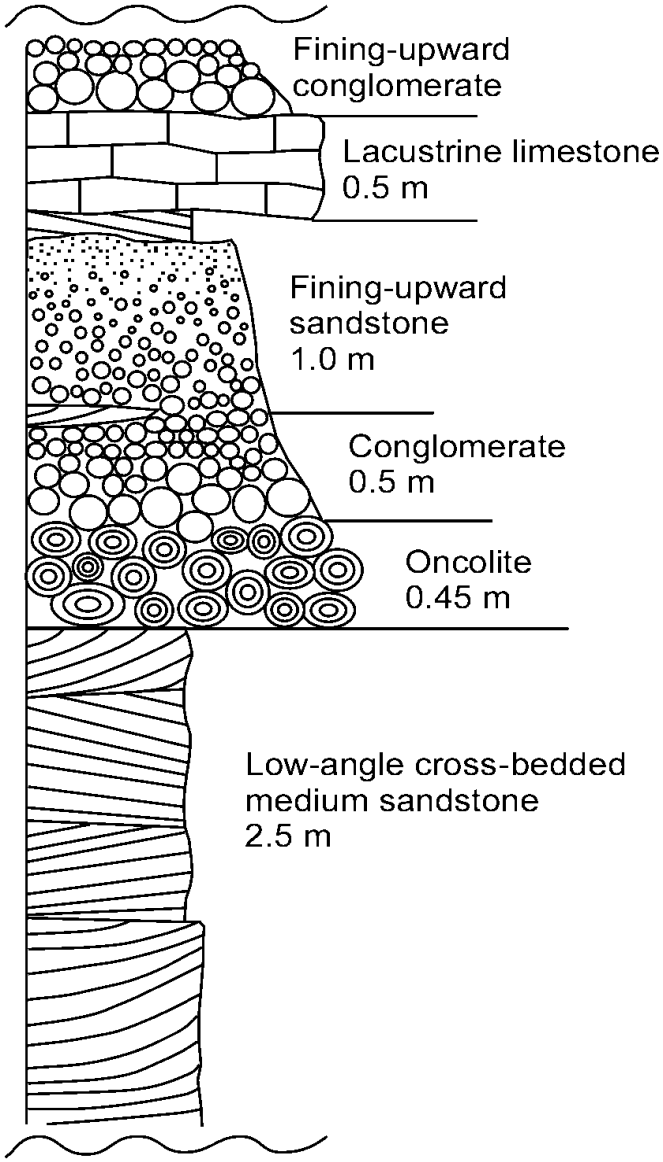

FIGURE 2—Simplified stratigraphy of the oncolite and associated lithofacies directly overlying the Buckhorn Conglomerate Member. This idealized column is based on average thicknesses. In all sections, the contact with the underlying Buckhorn Conglomerate is sharp.

Swell of central Utah (Fig. 1). In this area of nearly complete exposure, the indurated BCM holds up ridges and stands out among the more easily weathered mudstones of the underlying Upper Jurassic Morrison Formation or the overlying members of the CMF. In the area of the oncoids, there is not a continuous vertical section of the BCM. Currie (1998) reports a thickness of ~16 m of BCM in the San Rafael Swell.

Detailed stratigraphic analysis from the Woodside Anticline area has yielded important clues toward interpreting the facies of the oncoid-bearing lower CMF (Fig. 2). Three lithofacies dominate the stratigraphy overlying the BCM and underlying the variegated mudstone of the Ruby Ranch Member: (1) ~2–4-m-thick, well-sorted, medium-grained sandstone with low to moderate angle cross-beds and very rare dinosaur bones; (2) ~0.5–2-m-thick, normal-graded beds that range from cobble-sized conglomerate at the base to gravel, or rarely sand-sized at top, with dinosaur bones locally common; and (3) ~0.5-m-thick lenses of medium gray micritic, massive limestone with rare ostracodes, charophytes, and ruby-red stringers and nodules of chert. These lithofacies are not laterally traceable beyond 10 m. Oncoids are found primarily in the basal 40–100 cm of the conglomeratic units with scattered oncoids higher up. One oncoid was found within the sandy lithofacies. The clast composition of these conglomerates—largely sandstone and limestone—is distinctly different from the underlying BCM (primarily chert), suggesting a hiatus during deposition of the CMF (see also Currie, 1998). We tentatively assign these beds to the Poison Strip Sandstone based on comparison with other CMF outcrops in and around the San Rafael Swell (cf. Currie, 1998; Kirkland and Madsen, 2007).

Collections of oncoid samples for petrographic and stable isotope analysis were made during Summer 2004 from an ~10-m-thick interval, directly overlying the BCM. Over 50 samples, ranging from fragments to aggradations of oncoids, were collected in the field. Locations were recorded with a handheld global positioning receiver. Orthogonal photographs of outcrops were used for measurements of oncoid sizes. Oncoid nuclei compositions were recorded in the field.

In the laboratory, petrographic analysis was carried out on both polished slabs and thick (40 μm) and thin (30 μm) petrographic sections. Photomicroscopy was carried out using a PaxCam mounted on both an Olympus BX-51 petrographic microscope and a Nikon Optiphot microscope with a Reliotron cathodoluminescence chamber. Measurements were performed with PaxIT! software (Midwest Information Systems, Inc., 2006). Samples were taken for analysis from slabbed oncoid samples using a Dremel drill with diamond-tipped bits. Carbon and oxygen isotope ratios of milligram-sized carbonate are reported as $\delta^{13}C$ and $\delta^{18}O$ values, where R is the ratio of ^{18}O to ^{16}O, and δ is $(R_{sample}/R_{standard} - 1)*1000‰$, and the standard is Vienna Pee Dee Belemnite for carbon and oxygen. $\delta^{18}O$ and $\delta^{13}C$ of carbonate were measured using an automated carbonate preparation device (Kiel-III) coupled to a Finnigan MAT 252 isotope ratio mass spectrometer at the University of Iowa. Powdered samples were reacted with dehydrated phosphoric acid under vacuum at 75°C in the presence of silver foil. The isotope ratio measurement was calibrated based on repeated measurements of isotope standards NBS-19, NBS-18, and in-house powdered carbonate standards. Analytical precision is ±0.1‰ for both $\delta^{18}O$ and $\delta^{13}C$ (1σ). The carbonate-CO_2 fractionation for the acid extraction is assumed to be identical to calcite.

RESULTS

Oncoid Petrology

The oncoids of the lower CMF are in a variety of sizes, reflecting the size of the nuclei, but retain a consistent microstructure in the cortices. In the field, oncoids are found in a bimodal population (Fig. 3). The majority range from ~2 cm to 5 cm diameter, with a mean of 3.4 cm. The larger group includes oncoids >25 cm diameter. The oncoids are light gray, subround to oblate, and the external form mimics the shape of the nucleus. Within one oncolite bed, ≤70% of the grains are coated, and random oncoids are found within the overlying conglomerate (Fig. 3B). A 10–15-cm-thick caliche crust overlies several of the oncoid beds. Very rare oncoids are found in cross-bedded sandstone. No oncoids were observed in lacustrine limestone either in the study area or at other locations in the lower CMF.

Nuclei are largely rounded but nonspherical chert clasts. Other nuclei include litharenite, polymict conglomerate, and limestone (Fig. 3C). Of special note are locally common nuclei of both abraded and nonabraded dinosaur bone and wood fragments (Fig. 3D). Dinosaur bones range up to 20 cm long. Most are broken; however, one oncoid coated a vertebral column with extended, fine processes. The dinosaur bones have not been identified but are tentatively assigned to therapods and ankylosaurs based on rough field comparisons to better-identified dinosaur caches elsewhere in the lower CMF.

Cortices are generally 3–5 mm thick, but rinds >30 mm thick were measured. Thickness around the oncoid is not consistent, with one side generally 2–3 times thicker than the opposing margin. Weiss and Roche (1988) described oncoids from the CMF on the Gunnison Plateau as irregular, laminated, and mossy. Laminae are penecint (partially enclosed) and circumscribe the entire oncoid. Individual laminae are either low relief (<0.05 mm high) and crenulated or built up into ministromatolites (Fig. 4). Laminae average 0.24 mm thick and show a moderate degree of inheritance (Figs. 4A–B). Ministromatolites average 4.2 mm wide (range = 2–6 mm wide) and 1.2 cm tall (Figs. 4C–D). The oncoids are nearly devoid of organic remains, like most microbialites. In one thin section, however, a densely interwoven mat of filaments was preserved, albeit poorly (Fig. 4F). The filaments are hollow with no partitions observed. The walls are thick (average = 6.7 μm), but the thickening may be due to diagenesis. The filament diameter averages 30.7 μm. These filaments were most likely produced by bacteria. While it is not possible to assign them to a higher taxonomic grouping, the filaments are putatively of a sulfide-oxidizing bacterium similar to the modern *Beggiatoa* or *Thioplaca* based on the orientation and size of the filaments (e.g., Kojima et al., 2003; Nikolaus et al., 2003).

Most of the oncoids show a moderate degree of diagenetic alteration, most notably by the coarsening of minerals. Some laminae have been replaced by fan-shaped crystal aggregates (Freytet and Verrecchia, 1999); the true, finely laminated nature is preserved under cathodoluminescence. Silicification is rare. Overall, the predominant petrofabric is a spongy micrite typical of post-Cambrian oncoids. Disseminated pyrite occurs both along lamination and more randomly scattered throughout the oncoid. Pyrite concentration increases around original voids.

Stable Isotope Ratios

Multiple samples from four oncoids, multiple samples from a typical lacustrine limestone, and one dinosaur bone were sampled and analyzed (Table 1). Carbon and oxygen isotope data are characterized by a cluster of relatively high isotope ratios with values ranging from −9.5‰ to −8.5‰ and −4.0‰ to −3.0‰ for $\delta^{18}O$ and $\delta^{13}C$, respectively, and a tail of samples characterized by a range of lower isotope ratios (with minimums of −11.0‰ and −8.5‰ for $\delta^{18}O$ and $\delta^{13}C$, respectively; see Fig. 5A). Focusing only on samples with the highest isotope ratios, overlap among oncoid-limestone specimens is limited (Fig. 5B). A weak positive correlation between $\delta^{18}O$ and $\delta^{13}C$ is observed for these same samples (Fig. 5B). The correlation coefficient is 0.70 if all of these samples are included, and it is 0.60 if the oncoid sample with the lowest isotope ratios is excluded.

DISCUSSION

Oncoids and Landscape Reconstruction

The lack of marine deposits of this age and the association with adjacent lacustrine deposits (e.g., massive limestone) suggest that a lake shoreface is the most likely environment of formation for the CMF oncoids. The asymmetrical laminations and irregular shapes of the oncoids suggests that the oncoids did not form as rolling aggregates in high-energy channels or shorelines but, rather, formed in place along the lake margin where fluvial gravels were deposited from a change in flow velocity (cf. Freytet and Plaziat, 1979; Dahanayake et al., 1985). In some respects, oncoid formation is more akin to pisoid formation in soils or caves. Locally common abraded dinosaur bones and wood fragments within the oncoids suggest transport prior to setting and oncoid formation. As oncolite is not composed entirely of coated grains and some oncoids are found in predominantly conglomeratic beds, it is possible some postaccretion transportation took place. The lack of abraded margins and fracture casts of cortices does not indicate significant postaccretion transport. In some cases, several of the oncoid layers are overlain by a nonmicrobial caliche crust, likely formed during lake drawdown. For an extensive caliche crust to form, the area needed to be subaerial. Whether the entire lake disappeared is unknown. In essence, this crust is analogous to marine beach rock that forms at the high-water mark in tropical regions where evaporation is high.

Considering these inferred environments of oncoid formation in the context of stacked lithofacies it is possible to reconstruct the broader nature of the Early Cretaceous landscape. The lateral discontinuity of facies and aerial distribution suggest a broad plain of ephemeral lakes during oncoid formation. Unit stacking suggests that lakes periodically emptied and were overrun by fluvial processes, which took place several times during the history of the ephemeral lake (Fig. 6). The times of prolonged submergence allowed for the establishment of microbial mats leading to extensive oncoid formation on cobbles that were sometimes wave winnowed.

Stable Isotope Geochemistry and Lake History

The overall pattern in oxygen and carbon ratios for oncoids and associated carbonates most likely represents a combination of primary isotope ratios (i.e., the cluster of higher values) and samples that have undergone diagenetic alteration to varying degrees under different geochemical conditions (Fig. 5A). These data can be compared to stable

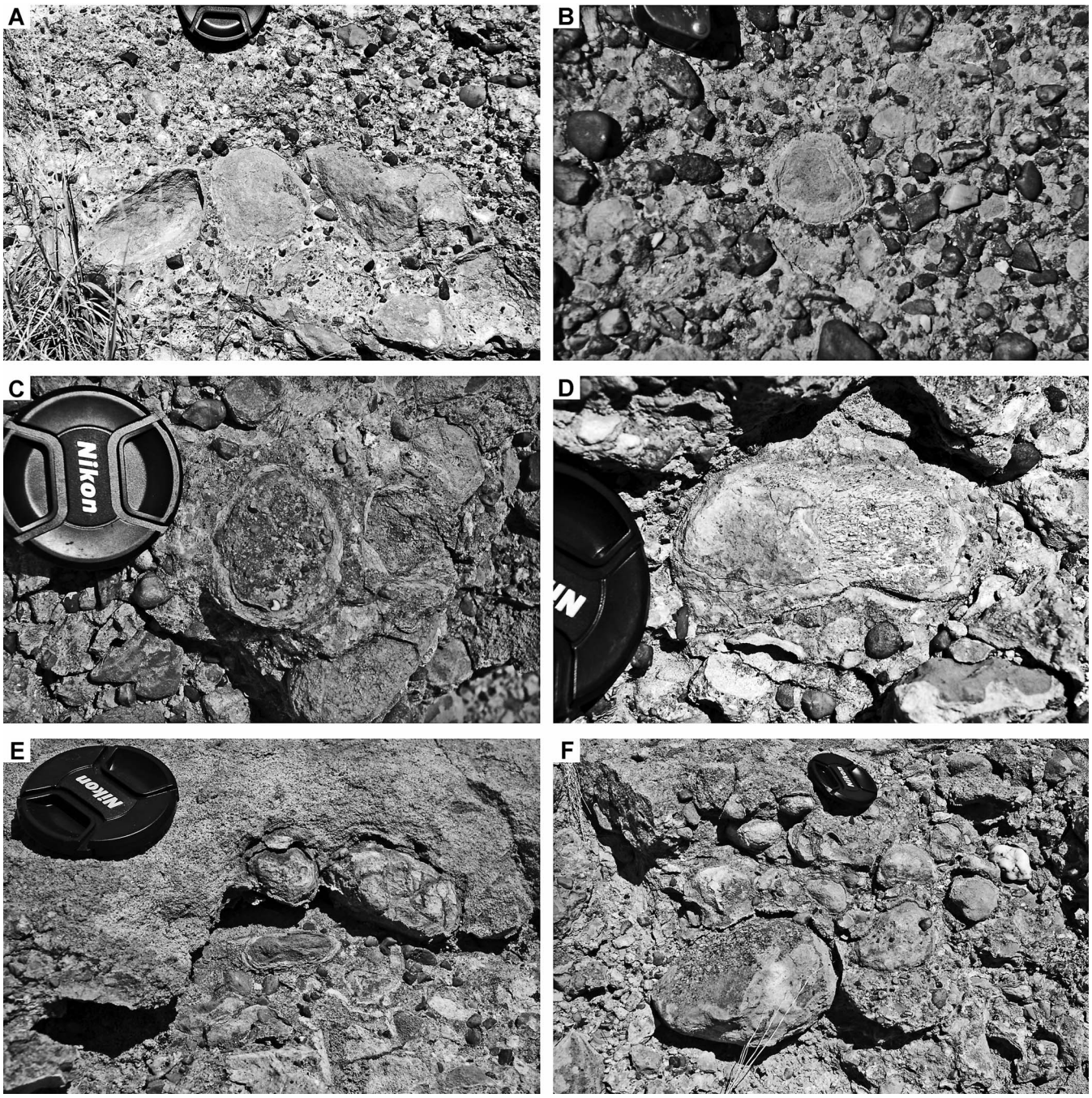

FIGURE 3—Field photographs of the oncolite in the Woodside Anticline. A) Larger oncoids overlain sharply by chert-rich conglomerate. B) Smaller oncoids entrained within chert-sandstone-limestone conglomerate; hand lens 2 cm wide. C) Exposed nucleus of the central oncoid is coarse sandstone, emphasizing the diversity of nuclei. D) Oncoid formed around an abraded dinosaur bone in a deposit of variable clast sizes. E) Cross section of the thick caliche enclosing the conglomerate, found only in the easternmost outcrops. F) Highly cemented oncolite with possible grading of the oncoids. Lens cap = 7 cm across.

isotope data from paleosol carbonates of the CMF of the same general area (Skipp, 1997) to provide a more complete interpretation of the CMF landscape.

In general, $\delta^{13}C$ values of our unaltered samples are higher than those of paleosol carbonates, whereas $\delta^{18}O$ vales are slightly lower (Fig. 5A). Paleosol carbonate $\delta^{13}C$ values are typical for the Late Jurassic–Early Cretaceous (e.g., Skipp, 1997; Ekart et al., 1999, and references therein). These values reflect oxidation of terrestrial organic matter in soil, diffusion and atmospheric CO_2 mixing, and precipitation of carbonate from groundwater in equilibrium with the soil CO_2 reservoir (Cerling, 1991). In contrast, higher $\delta^{13}C$ values of oncoids are consistent with formation in open, freshwater lakes (Talbot, 1990). In particular, $\delta^{13}C$ are interpreted to reflect multiple sources of carbon, including dissolved Paleozoic marine carbonate rocks in the watershed ($\delta^{13}C \sim 0‰$) and oxidized C_3 plant matter ($\delta^{13}C \sim -27‰$).

Oxygen isotope differences between groups of carbonate also point to a lacustrine origin for the oncoids. Paleosol carbonates form in equilibrium with soil waters (Cerling and Quade, 1993; Hsieh et al., 1998) that can have $\delta^{18}O$ values higher than mean annual because of (1) evaporative loss of water with ^{16}O to the atmosphere during dry seasons and (2) preferential formation of carbonates during these dry seasons. In contrast to soil water, lakes are much larger reservoirs that collect precipitation

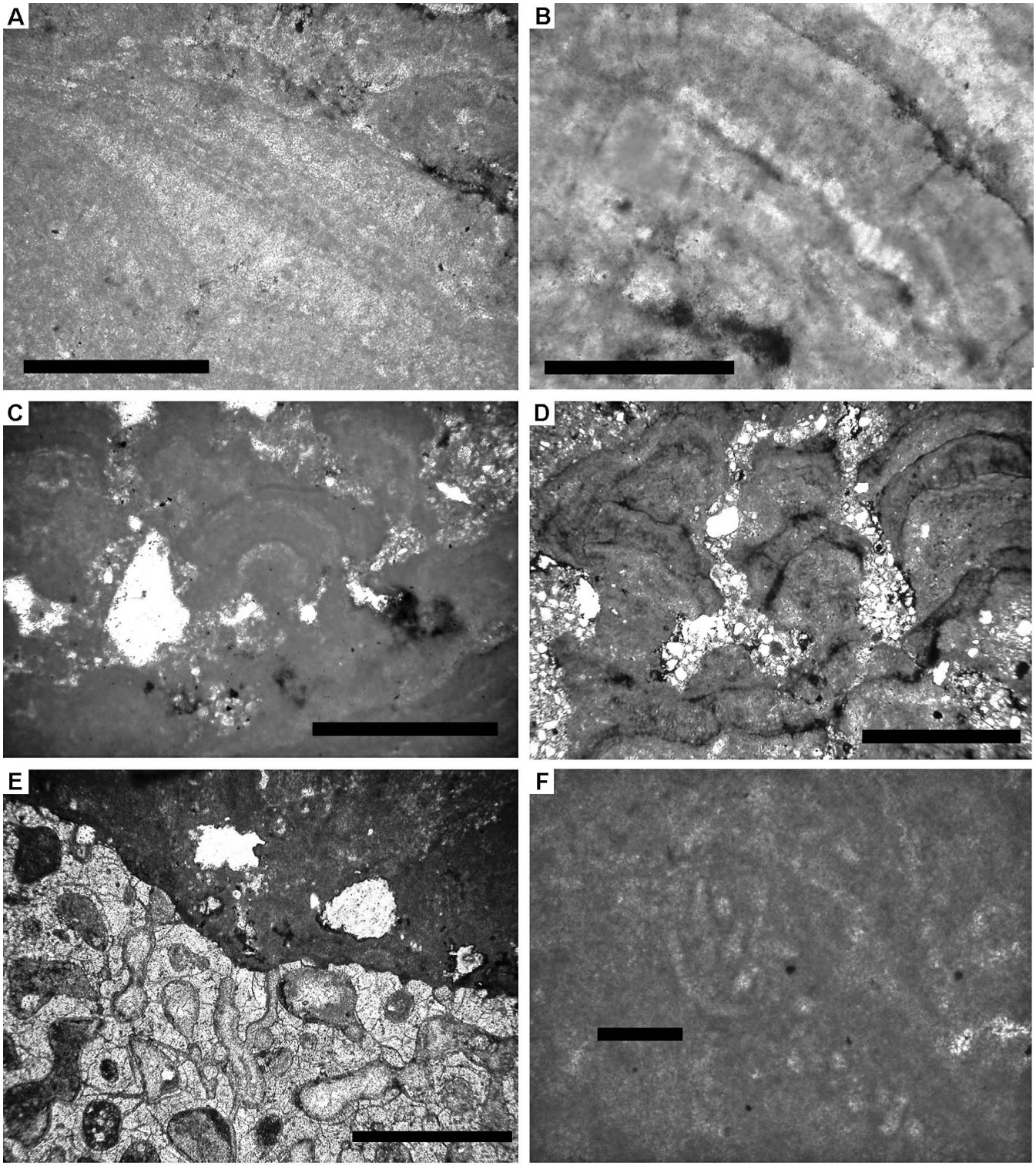

FIGURE 4—Photomicrographs of oncoid features. A) Detail of the laminae, showing crenulated texture. B) Doming of laminae that also shows diagenetic alteration in the form of pyrite-rich surfaces and fan-shaped crystal formation. C–D) Ministromatolites above domed laminae. Note detrital grains infilling between columns (plane polarized light). E) Oncoid grown on dinosaur bone, with pyrite at the pore boundaries (1/4 wave plate). F) Dense, interwoven bacterial? filaments within oncoid. Scale bar for A–C = 0.5 mm; D and E = 1 mm; F = 100 μm.

from the entire year, and modification of $\delta^{18}O$ due to evaporation is only a major factor for smaller ponds located in more arid environments (Talbot, 1990). The lower $\delta^{18}O$ of oncoids and associated carbonates compared to paleosols is, thus, consistent with their formation in medium to large lakes rather than smaller ponds or shallow soil settings.

Detailed evaluation of isotopic systematics of oncoids and associated carbonate indicates that evaporation of lake water took place, although evaporation does not appear to have had an extreme influence on lakes of the CMF where oncoids formed. First, for example, the weak positive correlation between $\delta^{18}O$ and $\delta^{13}C$ for all these samples (Fig. 5B; R^2 =

TABLE 1— Oxygen and carbon isotope data from oncoids and associated carbonates (this study) and from Early Cretaceous paleosol carbonates (Skipp, 1997; Fallin, 2005) use in Figure 5.

Sample	$\delta^{13}C$	$\delta^{18}O$	Symbol (Fig. 5B)
ONC A M1 GREY	−3.5	−8.8	diamond
ONC A M2 RED	−3.4	−8.8	diamond
ONC A M3	−3.6	−8.8	diamond
ONC B M1 7-3-04/15	−8.3	−11.0	n.a.
ONC B M2 7-3-04/15	−6.1	−10.5	n.a.
ONC C M1 7-1-04/1	−3.9	−8.7	triangle
ONC C M2 7-1-04/1	−3.8	−8.7	triangle
ONC CM3 RED 7-1-04/1	−3.7	−8.8	triangle
ONC D M1 7-16-04/10	−4.1	−9.5	square
ONC D M2 7-16-04/10	−3.9	−8.9	square
ONC D M3 7-16-04/10	−3.9	−8.8	square
ONC D M4 7-16-04/10	−3.8	−8.8	square
ONC E M1 7-3-04/10	−3.3	−8.5	cross
ONC E M2 7-3-04/10	−3.2	−8.4	cross
ONC F M1 7-16-04/3	−3.5	−8.5	circle
ONC F M2 7-16-04/3	−3.8	−8.7	circle

0.47) suggests that evaporation and organic productivity in the lake may have varied through time, with higher isotope ratios reflecting greater productivity during drier time periods (Talbot, 1990). Second, stable isotope ratios of altered samples reflect diagenetic conditions after burial, particularly the sample with the lowest $\delta^{18}O$ and $\delta^{13}C$ value (Lohmann, 1988). Low $\delta^{13}C$ values of diagenetic carbonate are consistent with carbon sourced from the oxidation of soil organic mater and incorporation of this carbon in groundwater. Low $\delta^{18}O$ values are again consistent with a meteoric water source, although values are ~2‰ lower than unaltered carbonate (Fig. 5A). Such an offset between primary lake and diagenetic carbonates could reflect (1) a higher temperature (by ~10°C) of formation from groundwaters having a $\delta^{18}O$ similar to lake water or (2) similar temperatures of formation of both primary and diagenetic carbonate, but with groundwaters having $\delta^{18}O$ ~ 2‰ lower than lake water. The latter would imply that $\delta^{18}O$ of lake water was shifted slightly to higher values relative to local meteoric water-precipitation that recharges groundwater. We prefer this latter interpretation given the sedimentological evidence for the limited size of these lakes and for the inferred episodic drying of them in this area during the Early Cretaceous.

Another interesting aspect of the oncoid $\delta^{18}O$ data is the relatively low values. $\delta^{18}O$ of ancient lake waters can be estimated by assuming temperatures of formation and using known isotopic fractionation factors for calcite and water (O'Neil et al., 1969). For a reasonable range of Early Cretaceous surface temperatures of 20–25°C, lake water is estimated to have been between ~ −6.5‰ and −7.5‰. A similar calculation using $\delta^{18}O$ from diagenetic and meteoric samples indicates that these waters have values of ~ −8.5‰ and −9.5‰. Regardless of whether precipitation or lake water in this area had $\delta^{18}O$ values of −7‰ or −9‰, these values are low compared to low-elevation localities at similar latitudes (~35°N) during both present-day (Dutton et al., 2005) and hothouse climate states (the Eocene; see Fricke, 2003). The implication of these lower $\delta^{18}O$ values is that rivers feeding the CMF lakes captured precipitation from high-elevation areas in the region. This inferred topographic relief is consistent with sedimentological evidence for high-energy rivers (i.e., conglomerates in the BCM) flowing from the Sevier orogenic belt.

CONCLUSIONS

The oncoid-bearing lacustrine deposits of the CMF described here help elucidate the Early Cretaceous landscape evolution in the area of the Woodside Anticline. Together with the underlying BCM, these rocks record the change from a classic continental fluvial succession, dominated by channel sandstone and floodplain deposits to lacustrine mudstone and limestone. The details of the oncoids record a unique situation where evaporation of small, ephemeral lakes preserved bacterial carbonates that coated rock fragments along the shore. Included in these fragments are

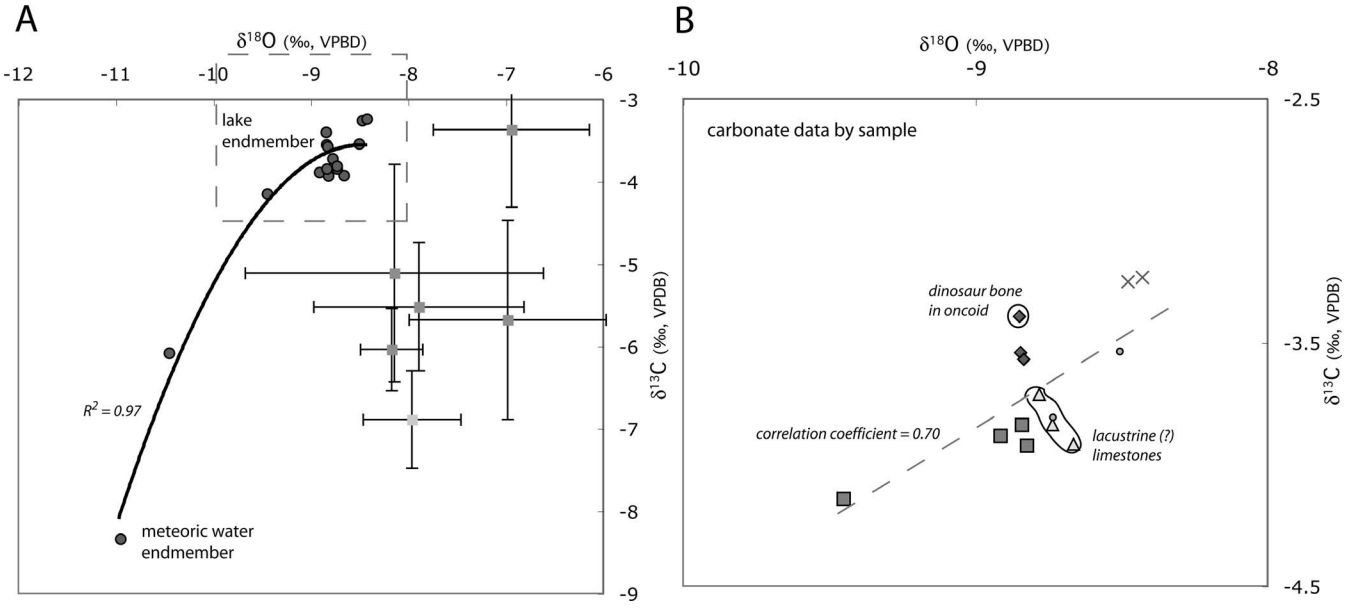

FIGURE 5—Oxygen and carbon isotope data from oncoids and associated carbonates (this study) and from Early Cretaceous paleosol carbonates (Skipp, 1997; Fallin, 2005). Data inside dashed box of A is highlighted in B. Data from this study is in circles. Black line is a second-order polynomial fit through these data. Lowest isotope ratios represent samples that underwent a larger degree of secondary exchange with diagenetic fluids of meteoric origin; samples with highest isotope ratios (dashed box) represent conditions of formation in CMF lakes. Paleosol carbonates from east-central Utah and west-central Colorado (solid squares ± 1 SD), and from the Bighorn Basin in Wyoming (hollow square ± 1 SD), generally have higher oxygen isotope ratios and lower oxygen isotope ratios than our samples. Each symbol represents samples from individual oncoids, a sample of a dinosaur bone at the core of an oncoid (circled), and from associated limestone (circled). Dashed line is a linear fit through the data. A correlation coefficient of 0.70 (0.60 excluding sample with lowest isotope ratios) reflects a positive correlation between carbon and oxygen isotope ratios of lake carbonates likely influenced by evaporative conditions in lakes.

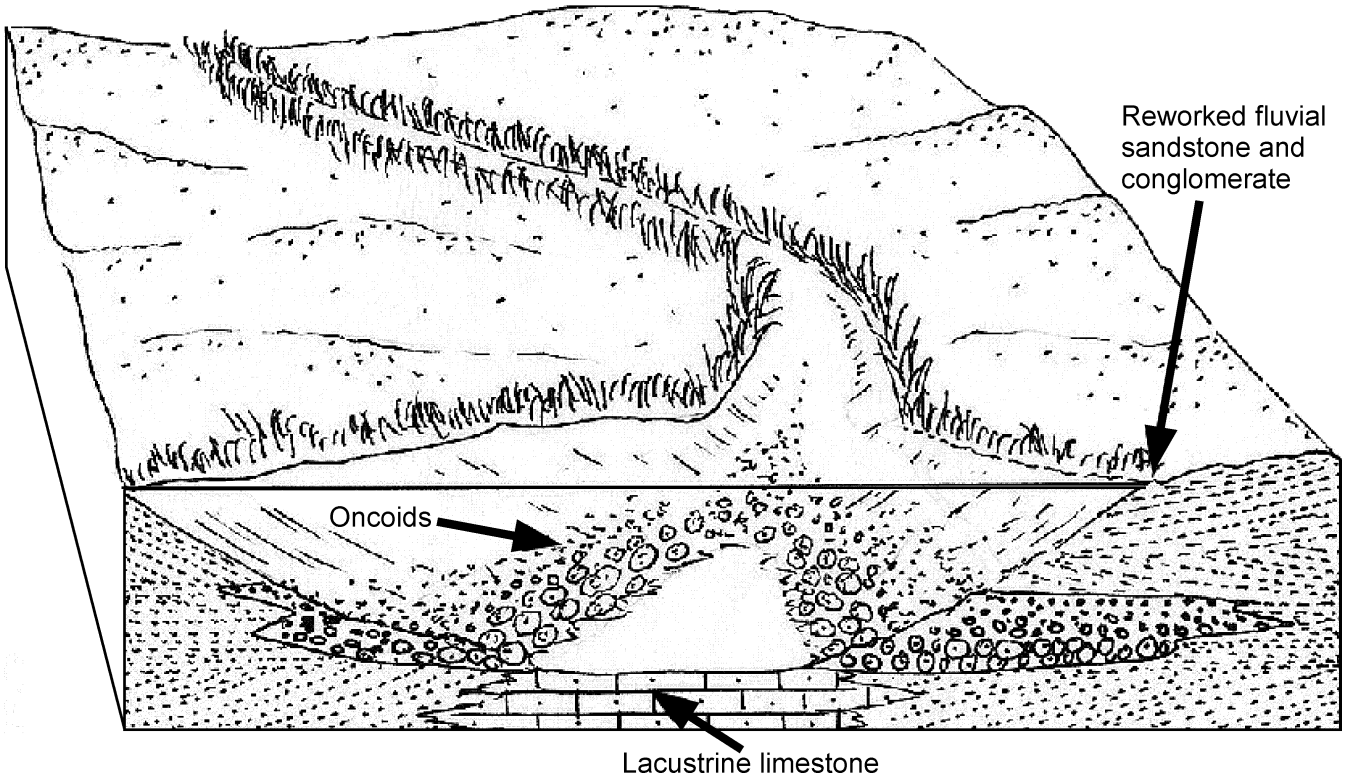

FIGURE 6—Reconstruction of the depositional environment showing a stream emptying into an ephemeral lake. Lime mud gathered in the deepest part of the lake. Coarse gravel is deposited where the river enters the lake. These gravels form the nuclei for the oncoids. Surrounding sediments are reworked fluvial sands and gravels.

dinosaur bones. Although constrained to the Woodside Anticline, the oncoids of the basal CMF further detail Early Cretaceous depositional environments as a series of ephemeral and evaporative lakes that formed on a braid plain of rivers originated from the Sevier highlands to the west.

ACKNOWLEDGMENTS

We thank Stephen Hasiotis, James Kirkland, and an anonymous reviewer for helpful comments and criticisms that greatly improved the manuscript. The field research was funded through an National Science Foundation Research Experiences for Undergraduates Reconstructing Rivers grant to Dr. Julie Maxson (Metropolitan State University, Minnesota).

REFERENCES

Awramik, S.M., Buchheim, H.P., Leggit, L., and Woo, K.S., 2000, Oncoids of the Late Pleistocene Manix Formation, Mojave Desert region, California: San Bernardino County Museum Association Quarterly, v. 47, p. 25–31.

Britt, B.B., Scheetz, R.D., Brinkman, D.B., and Eberth, D.A., 2006, A Barremian neochoristodere from the Cedar Mountain Formation, Utah, U.S.A.: Journal of Vertebrate Paleontology, v. 26, p. 1005–1008.

Cerling, T., 1991, Carbon dioxide in the atmosphere: Evidence from Cenozoic and Mesozoic paleosols: American Journal of Science, v. 291, p. 377–400.

Cerling, T.E., and Quade, J., 1993, Stable carbon and oxygen isotopes in soil carbonates, *in* Swart, P., Lohmann, K.C., McKenzie, J.A., and Savin, S., eds., Climate Change in Continental Isotopic Records: Geophysical Monograph, v. 78, p. 217–231.

Cifelli, R.L., Kirkland, J.I., Weil, A., Deinos, A.R., and Kowallis, B.J., 1997, High precision $^{40}Ar/^{39}Ar$ geochronology and the advent of North America's Late Cretaceous terrestrial fauna: Proceedings of the National Academy of Sciences USA, v. 94, p. 11,163–11,167.

Currie, B.S., 1998, Upper Jurassic–Lower Cretaceous Morrison and Cedar Mountain formations, NE Utah–NW Colorado; relationships between nonmarine deposition and early Cordilleran foreland-basin development: Journal of Sedimentary Research, v. 68, p. 632–652.

Dahanayake, K., Gerdes, G., and Krumbein, W.E., 1985, Stromatolites, oncolites and oolites biogenically formed *in situ*: Naturwissenchaften, v. 72, p. 513–518.

Davaud, E., and Girardclos, S., 2001, Recent freshwater ooids and oncoids from western Lake Geneva (Switzerland): Indications of a common organically mediated origin: Journal of Sedimentary Research, v. 71, p. 423–439.

DeCelles, P.G., and Coogan, J.C., 2006, Regional structure and kinematic history of the Sevier fold-and-thrust belt, central Utah: Geological Society of America Bulletin, v. 118, p. 841–864.

Demko, T.M., Currie, B.S., and Nicoll, K.A., 2004, Regional paleoclimatic and stratigraphic implications of paleosols and fluvial/overbank architecture in the Morrison Formation (Upper Jurassic), Western Interior, USA: Sedimentary Geology, v. 167, p. 115–135.

Dixit, P.C., 1984, Pleistocene lacustrine ridged oncolites from the Lake Manyara area, Tanzania, East Africa: Sedimentary Geology, v. 39, p. 53–62.

Dumitrescu, M., Brassell, S.C., Schouten, S., Hopmans, E.C., and Sinninghe Damste, J.S., 2006, Instability in tropical Pacific sea-surface temperatures during the early Aptian: Geology, v. 34, p. 833–836.

Dutton, A., Wilkinson, B.H., Welker, J.M., Bowen, G.J., and Lohmann, K.C., 2005, Spatial distribution and seasonal variation in $^{18}O/^{16}O$ of modern precipitation and river water across the conterminous USA: Hydrological Processes, v. 19, p. 4121–4146.

Ekart, D., Cerling, T., Montañez, I., Tabor, N., 1999, A 400 million year carbon isotope record of pedogenic carbonate: Implications for paleoatmospheric carbon dioxide: American Journal of Science, v. 299, p. 805–827.

Fallin, M.J., 2005, Carbon isotope stratigraphy of the Morrison and Cloverly Formations and assessment of vertical color change in the Morrison Formation, Coyote Basin: Unpublished M.S. thesis, University of Colorado, Boulder, 129 p.

Freytet, P., and Plaziat, J.C., 1979, Les ooides calcaires continentaux: Diversité des formes, des gisements, des modes de formation: Recherches Géographiques à Strasbourg, v. 12, p. 69–80.

Freytet, P., and Verrecchia, E.P., 1999, Calcitic radial palisadic fabric in freshwater stromatolites: Diagenetic and recrystallized feature or physicochemical sinter crust?: Sedimentary Geology, v. 126, p. 97–102.

Fricke, H.C., 2003, Investigation of early Eocene water-vapor transport and paleoelevation using oxygen isotope data from geographically widespread mammal remains: Geological Society of America Bulletin, v. 115, p. 1088–1096.

Hofmann, H.J., 1969, Attributes of stromatolites: Geological Society of Canada, Paper 69/39, 58 p.

Hsieh, J., Chadwick, O.A., Kelly, E., and Savin, S.M., 1998, Oxygen isotopic composition of soil water: Quantifying evaporation and transpiration: Geoderma, v. 82, p. 269–293.

Kirkland, J.I., Britt, B.B., Burge, D.L., Carpenter, K., Cifelli, R., DeCourten, F., Eaton, J., Hasiotis, S., and Lawton, T., 1997, Lower to middle Cretaceous dinosaur faunas of the central Colorado Plateau—A key to understanding 35 million years of tectonics, sedimentology, evolution, and biogeography: Brigham Young University Geology Studies, v. 42, pt. v. 2, p. 69–103.

Kirkland, J.I., Cifelli, R., Britt, B.B., Burge, D.L., DeCourten, F., Eaton, J., and Parrish, J.M., 1999, Distribution of vertebrate faunas in the Cedar Mountain Formation, east-central Utah, *in* Gillette, D., ed., Vertebrate Paleontology in Utah: Utah Geological Survey Miscellaneous Publication no. 99-1, p. 201–217.

Kirkland, J.I., Lucas, S.G., and Estep, J.W., 1998, Cretaceous dinosaurs of the Colorado Plateau, *in* Lucas, S.G., Kirkland, J.I., and Estep, J.W., eds., Lower to Middle Cretaceous Non-marine Cretaceous Faunas: New Mexico Museum of Natural History and Science Bulletin, v. 14, p. 67–89.

Kirkland, J.I., and Madsen, S.K., 2007, The Lower Cretaceous Cedar Mountain Formation, eastern Utah: The view up an always interesting learning curve, *in* Lund W.R., ed., Field Guide to Geological Excursions in Southern Utah, Geological Society of America Rocky Mountain Section 2007 Annual Meeting [CD-ROM]: Utah Geological Association Publication no. 35, p. 1–108.

Kirkland, J.I., Zanno, L.E., Sampson, S.D., Clark, J.M., and DeBlieux, D.D., 2005, A primitive therizinosauroid dinosaur from the Early Cretaceous of Utah: Nature, v. 435, p. 84–87.

Kojima, H., Teske, A., and Fukui, M., 2003, Morphological and phylogenetic characterizations of freshwater *Thioploca* species from Lake Biwa, Japan, and Lake Constance, Germany: Applied and Environmental Microbiology, v. 69, p. 390–398.

Lanes, S., and Palma, R.M., 1998, Environmental implications of oncoids and associated sediments from the Remoredo Formation (Lower Jurassic), Mendoza, Argentina: Palaeogeography, Palaeoclimatology, Palaeoecology, v. 140, p. 357–366.

Lohmann, K.C., 1988, Geochemical patterns of meteoric diagenetic systems and their applications to the study of paleokarst, *in* James, N.P., and Choquette, P.W., eds., Paleokarst: Springer-Verlag, New York, p. 58–80.

Midwest Information Systems, Inc., 2006, PAX-it! software version 6.0, Villa Park, Illinois.

Nikolaus, R., Ammerman, J.W., and MacDonald, I.R., 2003, Distinct pigmentation and trophic modes in *Beggiatoa* from hydrocarbon seeps in the Gulf of Mexico: Aquatic Microbial Ecology, v. 32, p. 85–93.

O'Neil, J.R., Clayton, R.N. and Mayeda, T.K., 1969, Oxygen isotope fractionation in divalent metal carbonates: Journal of Chemical Physics, v. 51, p. 5547–5558.

Peryt, T.M., ed., 1983, Coated Grains: Springer-Verlag, Berlin, 668 p.

Ratcliffe, K.T., 1988, Oncoids as environmental indicators in the Much Wenlock Limestone Formation of the English Midlands: Journal of the Geological Society (London), v. 145, p. 117–124.

Roca, X., and Nadon, G.C., 2007, Tectonic control on the sequence stratigraphy of nonmarine retroarc foreland basin fills: Insights from the Upper Jurassic of central Utah, U.S.A.: Journal of Sedimentary Research, v. 77, p. 239–255.

Rouchy, J.M., Camoin, G., Casanova, J., and Deconinck, J.F., 1993, The central palaeo-Andean basin of Bolivia (Potosi area) during the Late Cretaceous and early Tertiary: Reconstruction of ancient saline lakes using sedimentological, paleoecological and stable isotope records: Palaeogeography, Palaeoclimatology, Palaeoecology, v. 105, p. 179–198.

Skipp, G., 1997, Characterization and paleoenvironmental interpretation of pedogenic carbonate at the J-K boundary, east-central Utah and west-central Colorado: Unpublished master's thesis, Colorado School of Mines, Golden, Colorado, 104 p.

Sprinkel, D.A., Weiss, M.P., Fleming, R.W., and Waanders, G.L., 1999, Redefining the Lower Cretaceous stratigraphy within the central Utah foreland basin: Utah Geological Survey, Special Study no. 97, 21 p.

Stokes, W.L., 1949, Morrison and related deposits in and adjacent to the Colorado Plateau: Geological Society of America Bulletin, v. 55, p. 951–992.

Stokes, W.L., 1952, Lower Cretaceous in Colorado Plateau: American Association of Petroleum Geologists Bulletin, v. 36, p. 1766–1776.

Suarez, M.B., Suarez, C.A., Kirkland, J.I., González, L.A., Grandstaff, D.E., and Terry, D.O., Jr., 2007, Sedimentology, stratigraphy, and depositional environment of the Crystal Geyser Dinosaur Quarry, East-Central Utah: PALAIOS, v. 22, p. 513–527.

Talbot, M.R., 1990, A review of the palaeohydrological interpretation of carbon and oxygen isotopic ratios in primary lacustrine carbonates: Isotope Geoscience, v. 80, p. 261–279.

Tucker, M.E., and Wright V.P., 1990, Carbonate Sedimentology: Blackwell Science, Oxford, UK, 496 p.

Weiss, M.P., and Roche, M.G., 1988, The Cedar Mountain Formation (Lower Cretaceous) in the Gunnison Plateau, central Utah, *in* Schmidt, C.J., and Perry, W.J., eds., Interaction of the Rocky Mountain foreland and Cordilleran thrust belt: Geological Society of America Memoir no. 171, p. 557–569.

White, T., Witzke, B., Ludvigson, G., and Brenner, R., 2005, Distinguishing base-level change and climate signals in a Cretaceous alluvial sequence: Geology, v. 33, p. 13–16.

Zakharov, Y.D., Smyshlyaeva, O.P., Tanabe, K., Shigeta, Y., Maeda, H., Ignatiev, A.V., Velivetskaya, T.A., Afanasyeva, T.B., Popov, A.M., Golozubov, V.V., Kolyada, A.A., Cherbadzhi, A.K., and Moriya, K., 2005, Seasonal temperature fluctuations in the high northern latitudes during the Cretaceous Period; isotopic evidence from Albian and Coniacian shallow-water invertebrates of the Talovka River basin, Koryak Upland, Russian Far East: Cretaceous Research, v. 26, p. 113–132.

ACCEPTED JULY 30, 2008